Anisotropic magnetoconductance of a InAs nanowire: Angle-dependent suppression of one-dimensional weak localization

Dong Liang, Juan Du, and Xuan P. A. Gao*
Department of Physics, Case Western Reserve University, Cleveland, Ohio 44106, USA
(Received 4 November 2009; revised manuscript received 28 February 2010; published 16 April 2010)

The magnetoconductance of an InAs nanowire is investigated with respect to the relative orientation between external magnetic field and the nanowire axis. It is found that both the perpendicular and the parallel magnetic fields induce a positive magnetoconductance. Yet the parallel magnetic field induced longitudinal magnetoconductance has a smaller magnitude. This anisotropic magnetotransport phenomenon is studied as a function of temperature, magnetic field strength, and at an arbitrary angle between the magnetic field and the nanowire. We show that the observed effect is in quantitative agreement with the suppression of one-dimensional weak localization.

DOI: 10.1103/PhysRevB.81.153304 PACS number(s): 73.63.Nm, 72.20.My, 73.20.Fz

In the past two decades, semiconductor nanowires have attracted much attention due to their great potential in both fundamental research and novel device applications. They are considered as versatile building blocks for future nanoelectronics,[1,2] and as a platform to explore the fundamental physical properties of quasi-one-dimensional (1D) (Refs. 3 and 4) or zero-dimensional system.[5–11] Moreover, the quasi-1D nature of semiconductor nanowires may help to achieve significant enhancement in thermoelectric performance.[12–14] Thus, it is highly desirable to investigate the quasi-1D transport properties of nanowire devices. Previously, transport studies on nanowire structures have shown interesting effects related to the quasiballistic transport,[3] quantum confinement,[4] and interference[15] effects. Magnetotransport studies also revealed various quantum transport phenomena such as 1D weak-localization or weak-antilocalization effect.[16–20] These results exemplify the wide range of possibilities to study nanoscale physics in semiconductor nanowire materials made by direct chemical synthesis.

Here, a comprehensive magnetotransport study is reported on a single InAs nanowire field-effect-transistor device. An anisotropic magnetoconductance is observed with regard to the orientation between the magnetic field and the nanowire axis. We show that this effect can be attributed quantitatively to the suppression of 1D weak-localization correction to nanowire conductance. While much work to date has been focused on studying the magnetoconductance of nanowires in perpendicular[16–20] or occasionally, parallel magnetic field,[21,22] we report the first measurement of the continuous evolution between the transverse and the longitudinal magnetoconductance, and show that the anisotropic magnetoconductance is explained by the 1D weak-localization model.[23,24]

InAs nanowires with 20 nm diameters were grown on silicon wafer in a thermal chemical-vapor deposition system. Nanowires were sonicated by ultrasound sonication and suspended in ethanol which was then dropped on silicon substrate with a thermal oxide layer on the surface for device fabrication. The 600-nm-thick oxide on silicon substrate was used as the gate dielectric and the highly doped n-type Si substrate itself was used as the gate electrode. Ti/Al(2 nm/60 nm) electrodes with 2 μm spacing were evaporated on both sides of nanowire to serve as source and drain contacts. The device was dipped in buffered hydrofluoric acid solution for about 3s before metal evaporation to remove any native oxide and ensure ohmic contacts. The two-terminal conductance (G) of the nanowire was measured by low-frequency lock-in amplifier at a constant excitation voltage of 1 mV. The magnetotransport measurement on the single InAs nanowire was performed in a Quantum Design physical property measurement system equipped with a rotating sample stage. Prior to cool down, the device was carefully aligned to make sure the axis of nanowire is parallel to the fixed magnetic field direction (the misalignment is within a few degrees). Then the computer-controlled rotator was used to rotate the nanowire to form an arbitrary angle between nanowire and the magnetic field B [see Fig. 3(a)].

The dependence of the InAs nanowire conductance G on the gate voltage V_g at various temperatures and zero magnetic field is shown in Fig. 1. The upper and bottom insets show the configuration and scanning microscope image of the device, respectively. The positive slope of $G(V_g)$ in Fig. 1 indicates that the carrier is n type, similar to reports in the literature.[25–29] In Fig. 1, it can be seen that the $G(V_g)$ curves shift downward as T decreases. This reduction in conductance was attributed to the weak-localization correction to

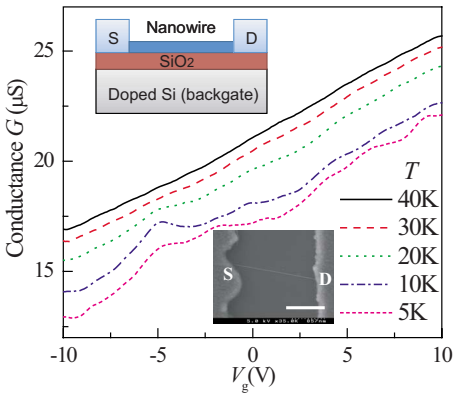

FIG. 1. (Color online) Dependence of conductance G on gate voltage of an InAs nanowire at temperature T=40, 30, 20, 10, and 5 K. Nanowire diameter is 20 nm. The top inset is a schematic of the nanowire device. The scanning electron microscope image of the device is shown as the bottom inset. The scale bar is 1 μm.

the Drude conductance instead of a decreasing carrier density effect.[20] Below 10 K, some small amplitude oscillations start to develop on top of the quasilinear $G(V_g)$ dependence. These oscillations are reminiscence of interference effects of electron waves undergoing multiple reflections inside the nanowire channel.[15] From the transconductance $g_m \equiv dG/dV_g$, we can estimate the electron mobility[29,30] $\mu = g_m \times L^2/C_g$, where C_g is the gate capacitance and $L=2$ μm is the length of nanowire between the electrodes. We can approximate the C_g with a wire on an infinite plate model and estimate electron mobility $\mu \approx 205$ cm^2/V s. The electron concentration can be roughly estimated as $n(V_g) = (V_g - V_{th})C_g/eL \approx (V_g - V_{th}) \times 280$ μm^{-1}. The threshold voltage V_{th} is ~ -45 V by linearly extrapolating the $G(V_g)$ curve to zero at $T=40$ K when the quantum correction to G is small. Thus, for the range of gate voltage studied (-10 to $+10$ V), electron concentration ranges from 1.0 to 1.5×10^4 μm^{-1}, or equivalently, 3.1 to 4.8×10^{19} cm^{-3}. For such high electron concentrations, there are many 1D subbands filled, therefore we use the three-dimensional (3D) formula to estimate the electron mean-free path $l \sim 13.1$, 14.4, and 15.2 nm, for $V_g = -10$, 0, and $+10$ V. The corresponding 3D Fermi wavelength λ_F is 6.5, 5.9, and 5.6 nm.

The magnetoconductance of nanowire is presented in Fig. 2(a) for both the perpendicular field and parallel field configurations at several temperatures from $T=40$ K down to 5 K. There are two main qualitative observations regarding the magnetoconductance $G(B)$. *First*, at $B<2$ T, both the perpendicular field ($B_\perp$) and parallel field ($B_\parallel$) induce a positive magnetoconductance, whose magnitude increases at lower temperature. The positive magnetoconductance in $B_\perp$ has been explained by the suppression of 1D weak localization by us in an earlier paper.[20] Above 2 T, the conductance of nanowire tends to saturate, due to the complete suppression of weak-localization effect.[20] *Second*, at all temperatures, the increment in $G(B_\perp)$ is always larger than $G(B_\parallel)$. This difference between the transverse magnetoconductance $G(B_\perp)$ and the longitudinal magnetoconductance $G(B_\parallel)$ is the main focus of this paper. Below we will show that both effects arise from the same mechanism, namely, magnetic field suppression of 1D weak localization.

Quantum correction to the Drude conductivity in weakly disordered system at low temperatures stems from weak localization, which is constructive quantum interference of time-reversal paths formed by diffusive electrons scattered elastically by impurities or defects.[31] Such weak-localization effects have been widely observed in various disordered electronic systems and received tremendous research interests.[32] One key parameter in this process is the phase-coherence length of electrons L_φ, indicating the characteristic length within which the electron maintains its phase coherence for the interference to take place. Phase coherence can be destroyed by electron-electron and electron-phonon scatterings. Such inelastic scatterings are strengthened by increasing temperature, which leads to the diminishing effect of the weak-localization effect at high temperatures. Moreover, magnetic field can be applied to introduce additional phase shifts to the electron waves traveling in time-reversed paths, which suppresses the weak localization and enhances the sample conductance. The dependence of conductance on

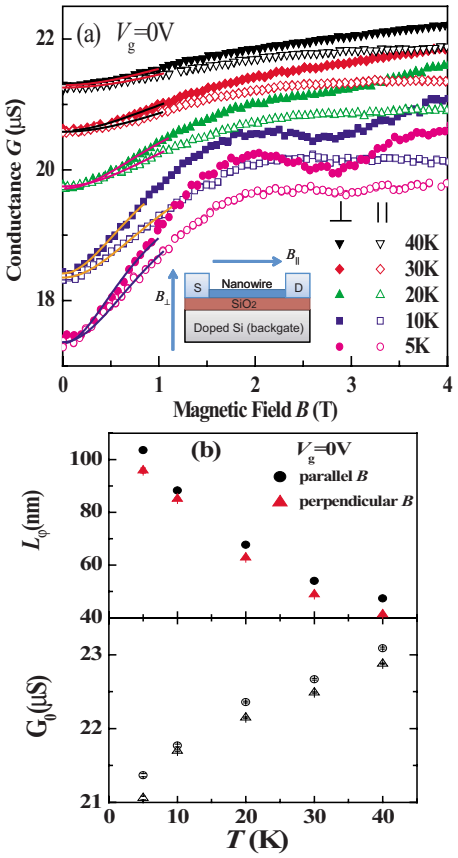

FIG. 2. (Color online) (a) InAs nanowire conductance vs magnetic field at temperature $T=40$, 30, 20, 10, and 5 K in $B_\perp$ (filled symbols) or $B_\parallel$ (open symbols). The gate voltage $V_g=0$ V. Solid curves show the best fits to 1D weak-localization theory. (b) The electron phase-coherence length L_φ and Drude conductance G_0 plotted as a function of temperature. L_φ and G_0 are obtained by fitting the low-field $G(B_\perp)$ or $G(B_\parallel)$ data to 1D weak-localization theory.

magnetic field is usually used to extract the L_φ. If $L_\varphi \gg w$, the width of system, the localization is regarded as 1D, and the quantum correction to conductance in magnetic field is given by the following equation:[23,24]

$$G(B) = G_0 - \frac{2e^2}{hL}\left(\frac{1}{L_\varphi^2} + \frac{1}{L_B^2}\right)^{-1/2}, \quad (1)$$

where $L=2$ μm is the length of the nanowire, $w=20$ nm is the width or diameter of nanowire, and G_0 is the classical Drude conductance. The magnetic relaxation length $L_B = (D\tau_B)^{1/2}$, with D as the diffusion constant and τ_B as the magnetic relaxation time which depends on the field orientation, strength, and wire cross-section shape, etc. We first fitted the low-field ($B<1$ T) $G(B_\perp)$ data in Fig. 2(a) to Eq. (1) using $L_B = L_{B\perp} = \sqrt{3}\hbar/(eB_\perp\sqrt{\pi(w/2)^2})$.[23,24,33] G_0 and L_φ are the only two fitting parameters. The fitting curves are indicated by the solid line in Fig. 2(a) while the fitted phase-coherence lengths L_φ and the Drude conductance G_0 at various temperatures are shown in Fig. 2(b). The above expression for $L_{B\perp}$ is applicable in the so-called "dirty metal" regime ($l \ll w$), and Eq. (1) requires $\sqrt{\hbar/eB} \gg w$ (the

weak-field limit). These requirements are satisfied reasonably for our parameters. As shown in the Fig. 2(b), L_φ, ranging from 41.3 to 103.6 nm, is much larger than the diameter w of the nanowire. This justifies the use of 1D weak localization ($L_\varphi > w$) to fit our data. It is interesting to note that the extracted G_0 has some temperature dependence. We believe that this residual T dependence in G_0 is due to the electron-electron interaction effects, which also give a correction to the Drude conductance.[18,22] It is well known that, unlike weak localization, electron-electron interaction-induced quantum correction to conductance is independent of magnetic field.[32] Thus, ignoring the electron-electron interaction correction[22] in our Eq. (1) will not affect our study of orientation-dependent $G(B)$, which is caused by the suppression of weak localization effect.

The weak-localization correction to the conductance of a wire in parallel magnetic field was also developed by Altshuler and Aronov.[23] The analytical expression is the same as Eq. (1) but with $L_B \equiv L_{B\|} = 2\sqrt{2}\hbar/(eB_\| w)$. We fit the $G(B_\|)$ in Fig. 2(a) to Eq. (1) using the expression for $L_{B\|}$ and found a good agreement. The extracted L_φ and G_0 are shown in Fig. 2(b) to compare with the results from fitting $G(B_\perp)$ data. There is a good agreement. Therefore, both the perpendicular- and parallel-field-induced magnetoconductance are consistent with the localization effect with the same parameters. Before we proceed to the angular dependence of $G(B)$, we like to make a few comments on the physical origin of the stronger $G(B)$ in the perpendicular configuration. Evidently, $L_{B\|} > L_{B\perp}$, this means that a perpendicular field is more effective than a parallel field in suppressing the localization effect. This difference is related to the 1D size confinement effect of coherent electron waves ($L_\varphi > w$). In the parallel field configuration, electron diffusion paths enclosing magnetic flux are well confined within the circumference of the nanowire while for the perpendicular field case, they are confined by nanowire diameter w in the radial direction and L_φ in the axial direction. So the magnetic fluxes enclosed by electron diffusion paths in perpendicular field are larger in the perpendicular field configuration. Thus, the additional phase shift introduced by a small magnetic field for $B_\perp$ is larger than $B_\|$, which leads to stronger suppression of weak-localization effect.

To further test the conclusion that the anisotropic magnetoconductance of our InAs nanowire has the same origin of magnetic field suppression of 1D weak localization, we carried out an angle-dependent experiment of the magnetoconductance at various temperatures in a fixed magnetic field of 1 T. The nanowire was carefully aligned to make sure it could be rotated about the axis perpendicular to both the magnetic field and the nanowire, as shown in Fig. 3(a) . The rotation angle θ is defined to be the angle between magnetic field and the cross-section plane of nanowire. The experimental data of angle dependence of magnetoconductance for $\theta = 0°$ to 360° are given in Fig. 3(b). The gate voltage V_g was set to 0 V. According to our definition of θ, B is exactly perpendicular to the nanowire at $\theta = 0°$ and 180°, and is exactly parallel to nanowire at $\theta = 90°$ and 270°. Obviously, since that magnetoconductance in perpendicular field is larger than in parallel field, $G(\theta)$ data in Fig. 3(b) shows peaks at 0°, 180°, and 360°, and dips at 90° and 270°. The

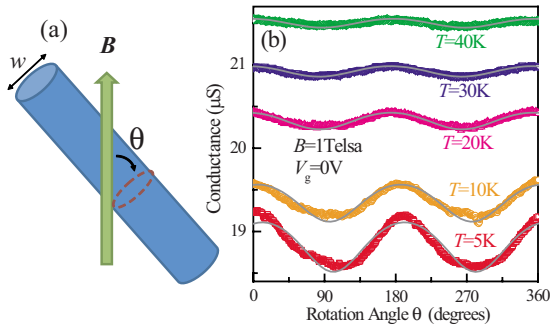

FIG. 3. (Color online) (a) Schematic of rotating a nanowire with diameter w in magnetic field B. Rotation angle θ is defined to be the angle between magnetic field and the cross section of nanowire. (b) Rotation-angle dependence of an InAs nanowire conductance at $V_g = 0$ V and $T = 40$, 30, 20, 10, and 5 K. Solid curves are the fits to Eq. (2).

small deviations of the peak and dip positions from 0°, 90°, 180°, and 270° may be caused by the misalignment of nanowire relative to magnetic field. In addition, the oscillatory amplitudes of $G(\theta)$ decrease as the temperature increases because of the weakening of the weak-localization effect at high temperatures. In order to explain the experimental data at an arbitrary angle θ, we decompose the magnetic field to a perpendicular component and a parallel component. These two orthogonal magnetic fields will both contribute to the suppression of electron localization in nanowire but with different magnitudes, as discussed earlier. The overall magnetoconductance is then given by

$$G(B,\theta) = G_0 - \frac{2e^2}{hL}\left(\frac{1}{L_\varphi^2} + \frac{1}{L_{B\perp}^2} + \frac{1}{L_{B\|}^2}\right)^{-1/2}. \qquad (2)$$

In Eq. (2), $L_{B\perp} = \sqrt{3}\hbar/(eB\cos\theta\sqrt{\pi(w/2)^2})$ and $L_{B\|} = 2\sqrt{2}\hbar/(ewB\sin\theta)$ are the magnetic relaxation lengths for the perpendicular and parallel components of B. The solid curves in Fig. 3(b) indicate the theoretical fits to Eq. (2), with G_0, L_φ fixed at the averaged values of data in Fig. 2(b), and a misalignment angle offset was set as the only free parameter. The fitted angle offset is within 10°. This good agreement between $G(\theta)$ data and theory further supports that the anisotropic magnetoconductance of nanowire is consistently explained by the 1D weak-localization theory.

In conclusion, angle dependence of the anisotropic magnetoconductance of a single InAs nanowire with 20 nm diameter is studied. The data are consistent with a modified model of magnetic field suppression of 1D weak localization where the magnetic field forms an arbitrary angle with the nanowire.[23,24] Similar angle-dependent magnetoconductance measurements on 1D quantum wires may be useful to explore other effects such as spin-orbit coupling effects in semiconductor nanowires.[34,35]

The authors thank K. Kash, M. MacDonald, H. Mathur, L. Qiu and R. S. Thompson for useful comments. X.P.A.G. acknowledges CWRU startup fund and ACS Petroleum Research Fund (Grant No. 48800-DNI10) for supporting this work.

*xuan.gao@case.edu

[1] W. Lu and C. M. Lieber, Nature Mater. **6**, 841 (2007).
[2] C. Thelander *et al.*, Mater. Today **9**, 28 (2006).
[3] W. Lu, J. Xiang, B. P. Timko, Y. Wu, and C. M. Lieber, Proc. Natl. Acad. Sci. U.S.A. **102**, 10046 (2005).
[4] S. R. Rustagi *et al.*, IEEE Electron Device Lett. **28**, 909 (2007).
[5] M. T. Björk, C. Thelander, A. E. Hansen *et al.*, Nano Lett. **4**, 1621 (2004).
[6] J. Xiang, A. Vidan, M. Tinkham, R. M. Westervelt, and C. M. Lieber, Nat. Nanotechnol. **1**, 208 (2006).
[7] Y. Hu, H. O. H. Churchill, D. J. Reilly, J. Xiang, C. M. Lieber, and C. M. Marcus, Nat. Nanotechnol. **2**, 622 (2007).
[8] C. Fasth, A. Fuhrer, L. Samuelson, V. N. Golovach, and D. Loss, Phys. Rev. Lett. **98**, 266801 (2007).
[9] S. Roddaro, A. Fuhrer, P. Brusheim, C. Fasth, H. Q. Xu, L. Samuelson, J. Xiang, and C. M. Lieber, Phys. Rev. Lett. **101**, 186802 (2008).
[10] F. A. Zwanenburg, C. E. W. M. van Rijmenam, Y. Fang, C. M. Lieber, and L. P. Kouwenhoven, Nano Lett. **9**, 1071 (2009).
[11] M. H. M. van Weert *et al.*, Nano Lett. **9**, 1989 (2009).
[12] L. D. Hicks and M. S. Dresselhaus, Phys. Rev. B **47**, 16631 (1993).
[13] A. I. Hochbaum *et al.*, Nature (London) **451**, 163 (2008).
[14] A. I. Boukai *et al.*, Nature (London) **451**, 168 (2008).
[15] A. T. Tilke, F. C. Simmel, H. Lorenz, R. H. Blick, and J. P. Kotthaus, Phys. Rev. B **68**, 075311 (2003).
[16] A. E. Hansen, M. T. Bjork, I. C. Fasth, C. Thelander, and L. Samuelson, Phys. Rev. B **71**, 205328 (2005).
[17] P. Lehnen, T. Schapers, N. Kaluza, N. Thillosen, and H. Hardtdegen, Phys. Rev. B **76**, 205307 (2007).
[18] F. J. Rueß, B. Weber, K. E. J. Goh, O. Klochan, A. R. Hamilton, and M. Y. Simmons, Phys. Rev. B **76**, 085403 (2007).
[19] S. Dhara, H. S. Solanki, V. Singh, A. Narayanan, P. Chaudhari, M. Gokhale, A. Bhattacharya, and M. M. Deshmukh, Phys. Rev. B **79**, 121311(R) (2009).
[20] D. Liang, M. R. Sakr, and X. P. A. Gao, Nano Lett. **9**, 1709 (2009).
[21] J. P. Heremans, C. M. Thrush, Z. Zhang, X. Sun, M. S. Dresselhaus, J. Y. Ying, and D. T. Morelli, Phys. Rev. B **58**, R10091 (1998).
[22] R. S. Thompson, D. Li, C. M. Witte, and J. G. Lu, Nano Lett. **9**, 3991 (2009).
[23] B. L. Altshuler and A. G. Aronov, JETP Lett. **33**, 449 (1981).
[24] C. W. J. Beenakker and H. van Houten, Phys. Rev. B **38**, 3232 (1988).
[25] T. Bryllert, L. E. Wernersson, L. E. Froberg, and L. Samuelson, IEEE Electron Device Lett. **27**, 323 (2006).
[26] S. A. Dayeh, D. P. R. Aplin, X. T. Zhou, P. K. L. Yu, E. T. Yu, and D. L. Wang, Small **3**, 326 (2007).
[27] X. Jiang, Q. Xiong, S. Nam, F. Qian, Y. Li, and C. M. Lieber, Nano Lett. **7**, 3214 (2007).
[28] A. C. Ford, J. C. Ho, Z. Fan, O. Ergen, V. Altoe, S. Aloni, H. Razavi, and A. Javey, Nano Res. **1**, 32 (2008).
[29] M. R. Sakr and X. P. A. Gao, Appl. Phys. Lett. **93**, 203503 (2008).
[30] J. Du, D. Liang, H. Tang, and X. P. A. Gao, Nano Lett. **9**, 4348 (2009).
[31] G. Bergmann, Phys. Rep. **107**, 1 (1984).
[32] P. A. Lee and T. V. Ramakrishnan, Rev. Mod. Phys. **57**, 287 (1985).
[33] Original equation for the perpendicular field configuration was obtained for wires with square cross section in Ref. 23. We modified the equation to account for the circular cross section of nanowire.
[34] M. Scheid, M. Kohda, Y. Kunihashi, K. Richter, and J. Nitta, Phys. Rev. Lett. **101**, 266401 (2008).
[35] R. G. Nazmitdinov, K. N. Pichugin, and M. Valin-Rodriguez, Phys. Rev. B **79**, 193303 (2009).